

**Strategical design and synthesis of D-A-D-based quinolines for improved
WORM memory performance**

*Varghese Maria Angela,^a Deviendran Harshini,^a Predhanekar Mohamed Imran^b and
Samuthira Nagarajan ^{a*}*

^a Organic Electronics Division, Department of Chemistry, Central University of Tamil Nadu, Thiruvarur 610 005, India, E-mail: snagarajan@cutn.ac.in

^b Department of Chemistry, Islamiah College, Vaniyambadi 635 752, India

Table of content

1. Materials and methods	S3
2. Synthetic route for the compounds 1-14	S4
3. Synthesis and analytical data of compounds.....	S5-S7
4. ^1H , ^{13}C NMR, and HRMS spectra of the synthesized compounds.....	S7-S17
5. Thin film analysis of the compounds 14a-d	S18
6. Electrochemical studies of the compounds 14a-d	S18
7. Computational studies of the compounds 14a-d	S19-S23
8. Memory device characterizations.....	S22-S23

1. Materials and methods

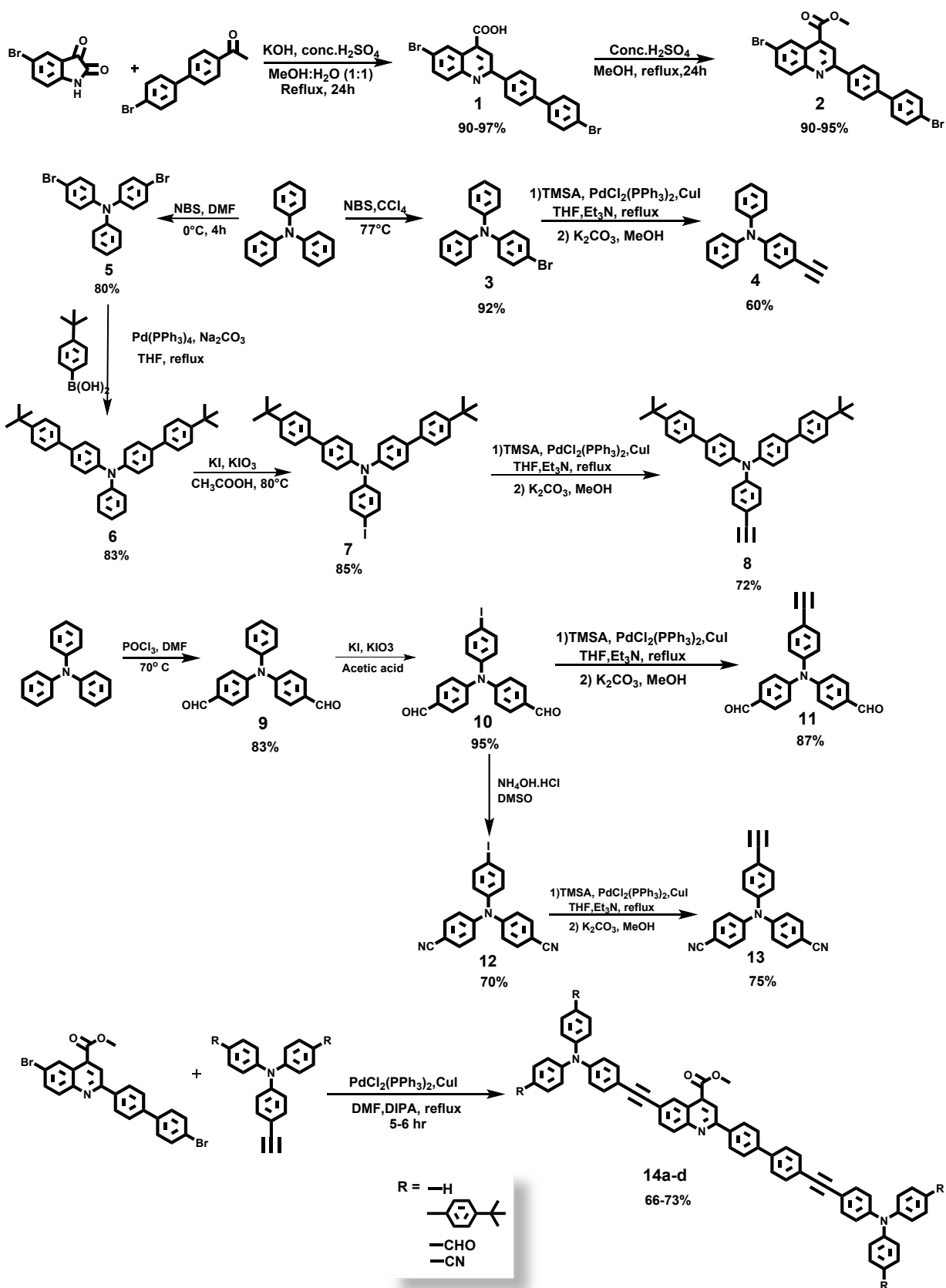
5-Bromoisatin, triphenylamine, bis(triphenylphosphine)palladium(II) dichloride, copper iodide, trimethylsilylacetylene, N-bromosuccinimide, tetrakis(triphenylphosphine)palladium, tertiary-butylphenylboronic acid, potassium iodide, potassium iodate, acetophenone, 4-fluoroacetophenone, 4-acetylanisole, dimethylformamide, tetrahydrofuran, triethylamine, diisopropylamine, were obtained from commercial sources and utilized as supplied unless otherwise specified. All of the solvents utilized were of ACS quality. The nitrogen atmosphere was maintained for all the Pd-catalysed reactions. Thin-layer chromatography was used to monitor the reactions, and column chromatography on silica columns with a mesh size of 100 – 200 was used to purify the products.

Tetramethylsilane (TMS) was used as the internal standard while recording the ¹H and ¹³C NMR spectra in a Bruker 400 MHz spectrometer. CHN elemental analysis was recorded on a Perkin-Elmer CHN 2400 analyzer. Thermo Exactive Plus UHPLC-MS provided high-resolution mass spectra. The JASCO UV-NIR spectrophotometer and the Perkin-Elmer LS 55 spectrophotometer were used to record the absorption and emission spectra. Electrochemical studies were performed in an electrochemical workstation (CHI 6035D). Surface morphology was determined by a VEGA3 TESCAN scanning electron microscope (SEM). DFT and TD-DFT studies were used to attain computational insights.

Fabrication and characterization of memory devices

The memory devices were fabricated by utilizing the synthesized compounds (**14a-d**) over an ITO-coated glass plate as the substrate. Distilled water, soap solution, acetone, and ethanol were used as sonicating agents for 10 minutes each to completely clean the ITO-covered glass plates. The target molecules are dissolved in chloroform solution (5 mg mL⁻¹) and spin-coated over the ITO-coated glass plate. After that, the thin film is annealed for 20 minutes at 80 °C. The device was then coated with silver contacts via sputtering using a mask of 1 mm dimension. The device was then utilized for the study of memory characteristics. Keithley 4200A semiconductor parameter analyzer was used to perform memory characterizations at ambient conditions.

2. Synthetic route for the targeted compounds



Scheme S1: Synthetic route for the compounds 1-14

3. Synthesis and analytical data of compounds

Compound 1: A 1:1 ratio of methanol and water (20 mL each) was initially used to dissolve 5-bromoisatin (1.5 g, 6.6 mmol). Potassium hydroxide (2.4 g, 4.4 mmol) was then added to the solution and stirred for 15 minutes till there is a color change from brown to pale yellow followed by the addition of 2M H₂SO₄ (10 mL). To this solution, 4’-(4-bromophenyl) acetophenone (4.5 g, 16.5 mmol) was added and refluxed for 32 hours. The reaction mixture was then added to cold water after the completion of the reaction. The precipitate formed was filtered off and then to the filtrate con. H₂SO₄ was added and filtered again to get the product. HRMS (ESI) (m/z): C₂₂H₁₃Br₂NO₂, Calc [M+H]⁺: 483.9326, Observed [M+H]⁺: 483.9355.

Compound 2: To compound **1** (3.0 g, 6.6 mmol) dissolved in methanol (25 mL), con. H₂SO₄ was added till the solution becomes miscible. The solution was stirred for 24 hours under reflux conditions. After the completion of the reaction, the reaction mixture was added to sodium bicarbonate to neutralize the solution and the product was obtained as a precipitate. The precipitate was then filtered and dried to get the product. ¹H NMR (400 MHz, CDCl₃) δ 8.99 (s, 1H), 8.54 (s, 1H), 8.41 (d, J = 8.0 Hz, 2H), 8.23 (s, 1H), 8.06 (dd, J = 19.6, 8.0 Hz, 1H), 7.75 (d, J = 8.0 Hz, 2H), 7.62-7.58 (m, 3H), 4.10 (s, 3H). ¹³C NMR (100 MHz, CDCl₃) δ 132.07, 129.04, 128.85, 128.73, 128.16, 127.69, 127.58, 127.06, 125.92, 121.66, 121.30, 105.84, 53.15.

The compounds **3**, **5-7**, **9**, **10**, and **12** were synthesized as per the reported procedures.¹

General procedure for Sonagashira coupling reaction of TAA acetylenes:

The halogenated triarylamine was dissolved in a 1:2 solution of anhydrous tetrahydrofuran (5 mL) and triethylamine (10 mL) followed by the addition of the palladium catalyst and copper sulphate respectively. This solution was purged with nitrogen for 15-20 minutes and then trimethylsilylacetylene was added by maintaining the nitrogen atmosphere under refluxing conditions. The product was purified using column chromatography and separated using hexane. The product was dissolved in methanol and potassium carbonate was then added and stirred for 2 hours at room temperature. The product was purified using column chromatography using hexane as the eluent.

Compound 4: Compound **3** underwent the general Sonagashira coupling procedure to give compound **4** a brown solid (60 %). ¹H NMR (400 MHz, CDCl₃) δ 7.27 – 7.24 (m, 2H), 7.22 – 7.16 (m, 5H), 7.02 (dd, J = 8.8, 1.2 Hz, 4H), 6.99 – 6.96 (m, 1H), 6.90 – 6.88 (m, 2H), 2.95 (s, 1H). ¹³C NMR (100 MHz, CDCl₃) δ 148.37, 147.13, 133.07, 129.42, 125.06, 123.65, 122.06, 114.75, 83.94.

Compound 8: Compound **7** underwent the general Sonagashira coupling procedure to give compound **8** as a brown powder (72 %). ¹H NMR (400 MHz, CDCl₃) δ 7.54 – 7.49 (m, 8H), 7.46 (d, J = 8.4 Hz, 4H), 7.39 – 7.36 (m, 2H), 7.19 – 7.17 (m, 4H), 7.08 – 7.06 (m, 2H), 3.04 (s, 1H), 1.36 (s, 18H). ¹³C NMR (100 MHz, CDCl₃) δ 150.03, 148.13, 146.01, 137.61, 136.23, 133.16, 127.89, 126.42, 125.76, 125.04, 122.50, 115.02, 83.93, 34.55, 31.39.

Compound 11: Compound **10** underwent the general Sonagashira coupling procedure to give compound **11** a brown solid (87 %). ¹H NMR (400 MHz, CDCl₃) δ 9.91 (s, 2H), 7.80 (d, J = 8.4 Hz, 4H), 7.49 (d, J = 8.4 Hz, 2H), 7.20 (d, J = 8.4 Hz, 4H), 7.12 (d, J = 8.4 Hz, 2H), 3.13

(s, 1H). ^{13}C NMR (100 MHz, CDCl_3) δ 190.57, 151.59, 145.94, 133.84, 131.76, 131.42, 126.02, 123.39, 119.31, 82.87, 78.04.

Compound 13: Compound **12** underwent the general Sonagashira coupling procedure to give compound **13** a brown solid (75 %). ^1H NMR (400 MHz, CDCl_3) δ 7.56 (d, $J = 8.8$ Hz, 4H), 7.49 (d, $J = 8.4$ Hz, 2H), 7.12 (d, $J = 8.8$ Hz, 4H), 7.07 (d, $J = 8.4$ Hz, 2H), 3.13 (s, 1H). ^{13}C NMR (100 MHz, CDCl_3) δ 149.81, 145.44, 133.99, 133.72, 125.93, 123.51, 119.67, 118.74, 106.56, 82.68, 78.22.

General procedure for the synthesis of compounds **14a-d**:

The dibromoquinoline **2** (250 mg, 0.43 mmol) along with $\text{PdCl}_2(\text{PPh}_3)_2$ (15 mg, 0.021 mmol) catalyst and copper sulphate (4.15 mg, 0.021 mmol) were dissolved in a 1:2 solution of anhydrous dimethylformamide (7 mL) and diisopropylamine (14 mL). This mixture was purged with nitrogen for 15-20 minutes. The corresponding triarylamine acetylene derivative was then added to the solution under a nitrogen atmosphere and refluxed for 6 hours. The progress of the reaction was monitored through thin layer chromatography and after completion, the solvent was removed and the product was purified using column chromatography in DCM: hexane solvent system.

Compound 14a: By following the general reaction procedure, compound **2** and **4** (258 mg, 0.95 mmol) reacts to give **14a** as greenish yellow powder (73 %). ^1H NMR (400 MHz, CDCl_3) δ 8.92 (s, 1H), 8.44 (s, 1H), 8.28 (d, $J = 8.4$ Hz, 2H), 8.16 (d, $J = 8.8$ Hz, 1H), 7.84 (d, $J = 8.8$ Hz, 2H), 7.72 (d, $J = 8.0$ Hz, 3H), 7.57 (dd, $J = 25.2, 8.4$ Hz, 7H), 7.43 (d, $J = 8.8$ Hz, 3H), 7.29 (t, $J = 7.6$ Hz, 7H), 7.15 – 7.02 (m, 13H), 4.10 (s, 3H). ^{13}C NMR (100 MHz, CDCl_3) δ 166.62, 156.12, 148.57, 148.27, 147.12, 141.35, 139.29, 137.73, 134.98, 132.75, 132.03, 130.30, 129.47, 128.73, 128.45, 127.96, 127.45, 125.16, 123.95, 123.73, 123.40, 122.08, 120.74, 115.53, 91.99, 88.93, 52.93. $\text{C}_{63}\text{H}_{43}\text{N}_3\text{O}_2$: Calc. C 86.57, H 4.96, N 4.81; Found C 86.54, H 4.95, N 4.80.

Compound 14b: By following the general reaction procedure, compound **2** and **8** (465 mg, 0.87 mmol) reacts to give **14b** as yellow powder (80 %). ^1H NMR (400 MHz, CDCl_3) δ 8.86 (s, 1H), 8.38 (s, 1H), 8.22 (d, $J = 8.4$ Hz, 2H), 8.10 (d, $J = 8.8$ Hz, 1H), 7.96 (d, $J = 8.4$ Hz, 4H), 7.62 (d, $J = 6.0$ Hz, 3H), 7.46 – 7.43 (m, 20H), 7.39 – 7.37 (m, 10H), 7.13 – 7.11 (m, 5H), 7.04 (d, $J = 8.8$ Hz, 5H), 4.03 (s, 3H), 1.29 (s, 36H). ^{13}C NMR (100 MHz, CDCl_3) δ 166.63, 156.16, 150.05, 148.61, 148.05, 147.86, 146.05, 144.94, 139.31, 139.13, 137.61, 136.32, 136.23, 136.02, 132.84, 132.69, 132.05, 130.33, 129.02, 128.74, 127.92, 127.90, 127.47, 127.16, 127.09, 126.42, 125.76, 125.15, 125.05, 123.68, 122.68, 122.54, 120.76, 116.13, 91.15, 88.47, 52.93, 34.55, 31.39, 26.72. $\text{C}_{103}\text{H}_{91}\text{N}_3\text{O}_2$: Calc. C 88.19, H 6.54, N 3.00; Found C 88.01, H 6.44, N 3.00.

Compound 14c: By following the general reaction procedure, compound **2** and **11** (312 mg, 0.95 mmol) reacts to give **14c** as brown powder (66 %). ^1H NMR (400 MHz, CDCl_3) δ 9.85 (s, 4H), 8.92 (s, 1H), 8.41 (s, 1H), 8.22 (d, $J = 8.8$ Hz, 2H), 8.11 (d, $J = 9.2$ Hz, 1H), 7.96 – 7.95 (m, 1H), 7.79 (dd, $J = 8.8, 2.0$ Hz, 2H), 7.76 – 7.74 (m, 6H), 7.66 (d, $J = 8.8$ Hz, 3H), 7.54 – 7.51 (m, 7H), 7.48 – 7.46 (m, 4H), 7.17 – 7.15 (m, 4H), 7.11 – 7.09 (m, 4H), 4.04 (s, 3H). ^{13}C

NMR (100 MHz, CDCl₃) δ 190.60, 166.51, 151.63, 148.74, 145.74, 141.51, 139.24, 137.62, 135.00, 133.45, 132.64, 132.05, 131.80, 131.46, 130.86, 130.44, 128.97, 128.73, 128.01, 127.48, 126.09, 123.94, 123.46, 122.71, 122.14, 120.88, 120.18, 90.64, 90.44, 52.95. C₆₇H₄₃N₃O₆: Calc. C 81.61, H 4.40, N 4.26; Found C 81.56, H 4.31, N 4.22.

Compound 14d: By following the general reaction procedure, compound **2** and **13** (306 mg, 0.95 mmol) react to give **14d** as a brown powder (69 %). ¹H NMR (400 MHz, CDCl₃) δ 9.00 (s, 1H), 8.49 (s, 1H), 8.31 (d, J = 8.4 Hz, 2H), 8.20 (d, J = 8.8 Hz, 1H), 7.87 (dd, J = 8.4, 1.6 Hz, 1H), 7.75 (d, J = 8.8 Hz, 3H), 7.63 – 7.54 (m, 17H), 7.17 – 7.12 (m, 10H), 4.11 (s, 3H). ¹³C NMR (100 MHz, CDCl₃) δ 166.50, 149.85, 148.78, 145.21, 141.55, 133.74, 133.59, 132.60, 132.05, 130.48, 129.02, 128.73, 128.01, 127.58, 127.50, 126.01, 125.92, 123.94, 123.56, 122.60, 122.15, 120.89, 120.56, 118.75, 106.60, 90.61, 90.39, 52.95. C₆₇H₃₉N₇O₂: Calc. C 82.61, H 4.04, N 10.07; Found C 82.44, H 4.01, N 10.02.

4. ¹H, ¹³C NMR, and HRMS spectra of the synthesized compounds

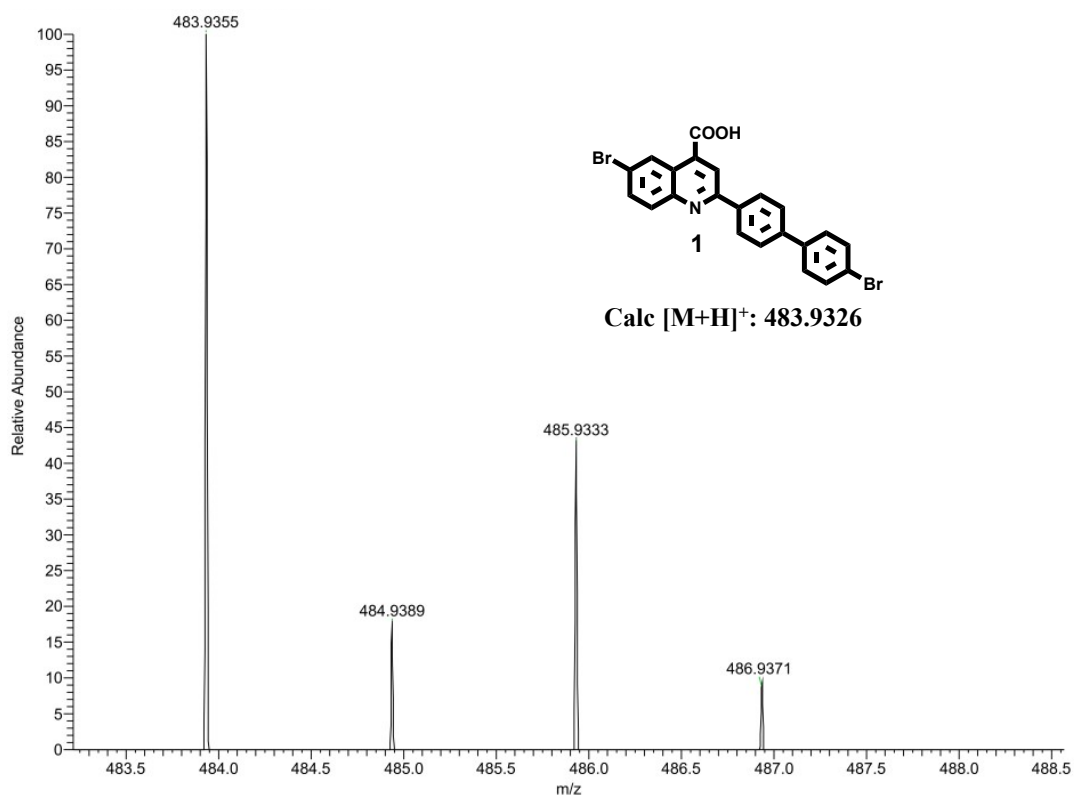


Figure S1: HRMS spectrum of compound **1**

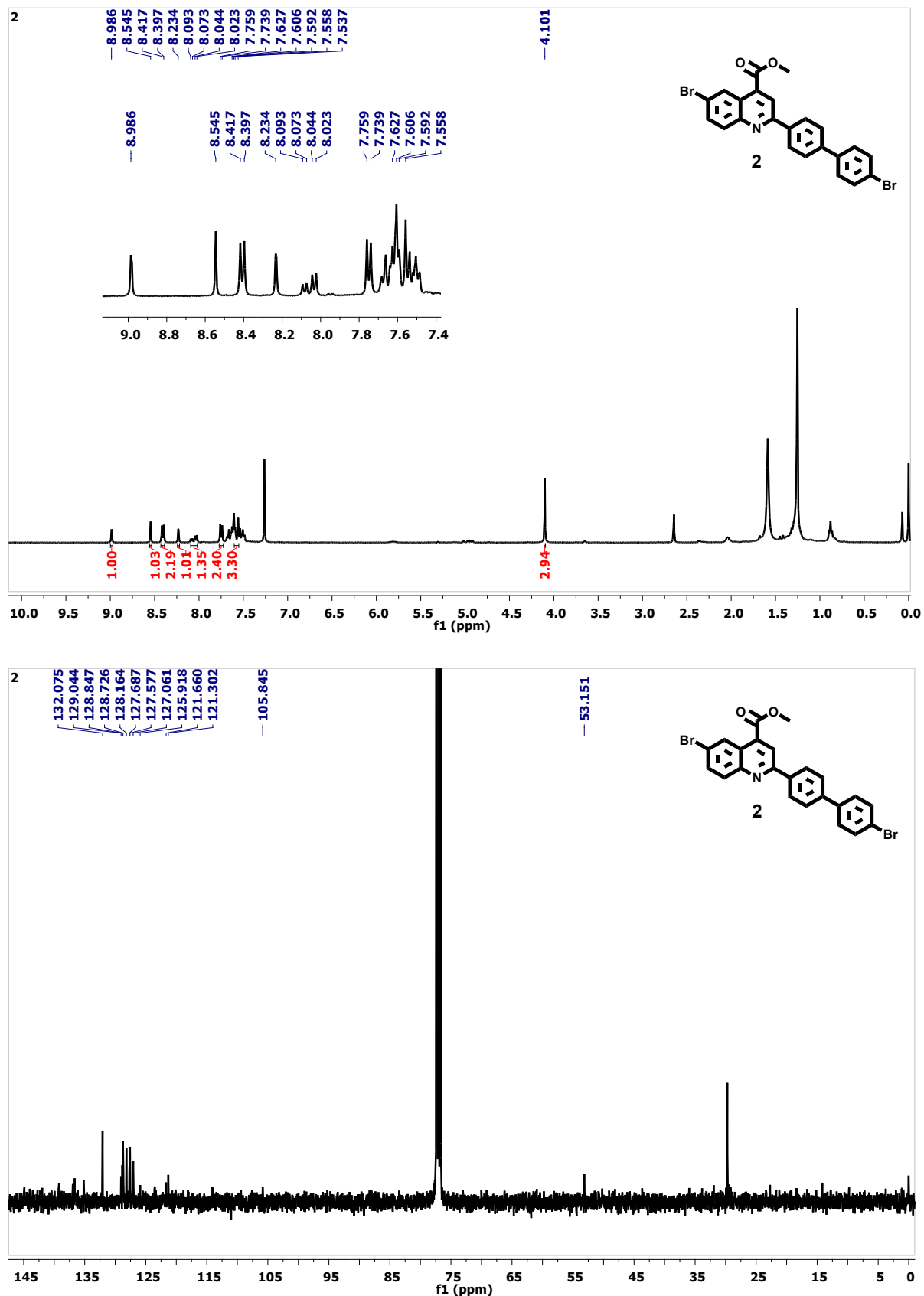


Figure S2: ^1H and ^{13}C NMR spectra of compound 2

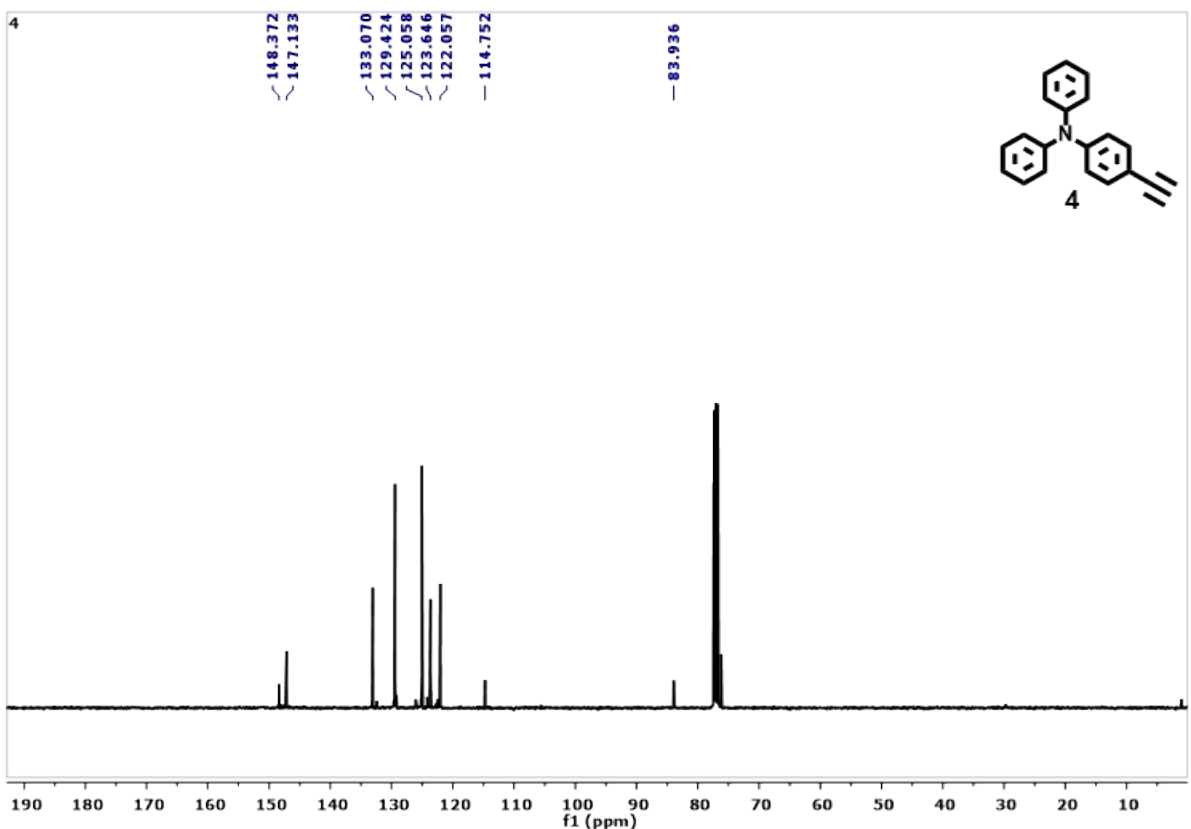
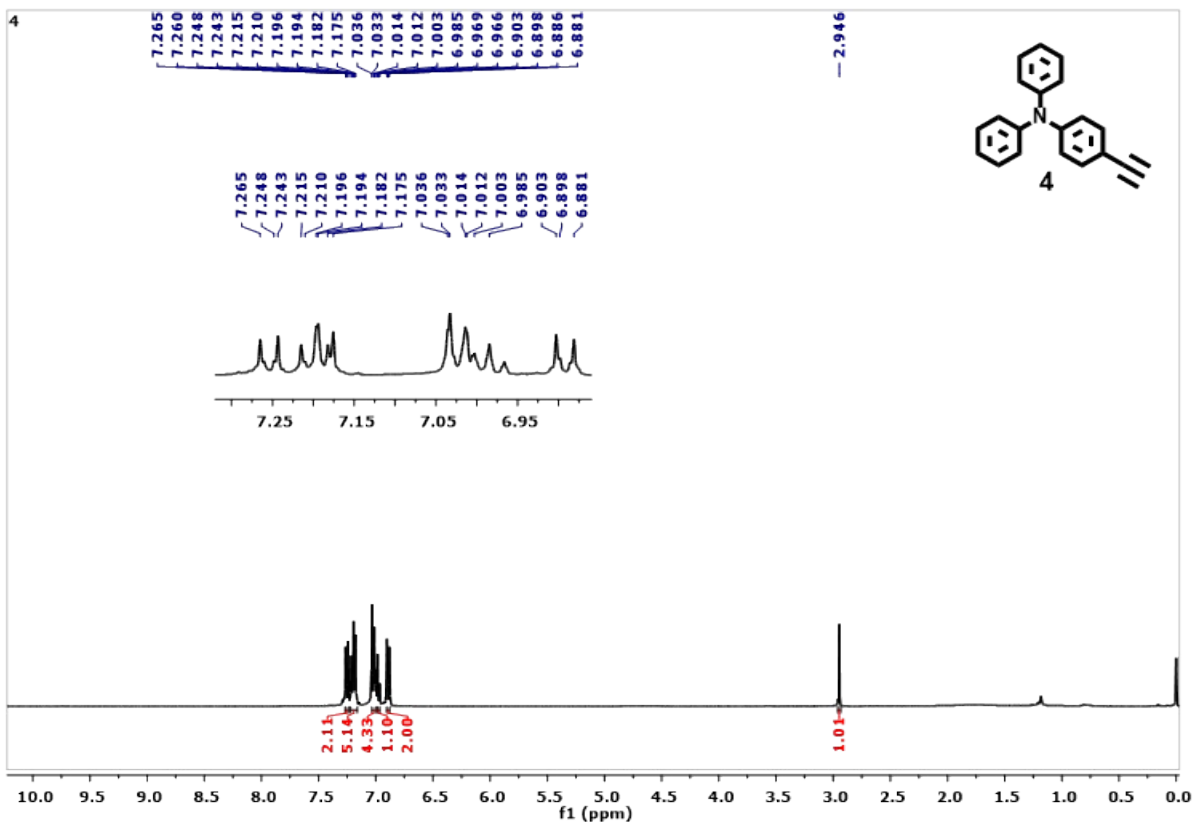


Figure S3: ^1H and ^{13}C NMR spectra of compound 4

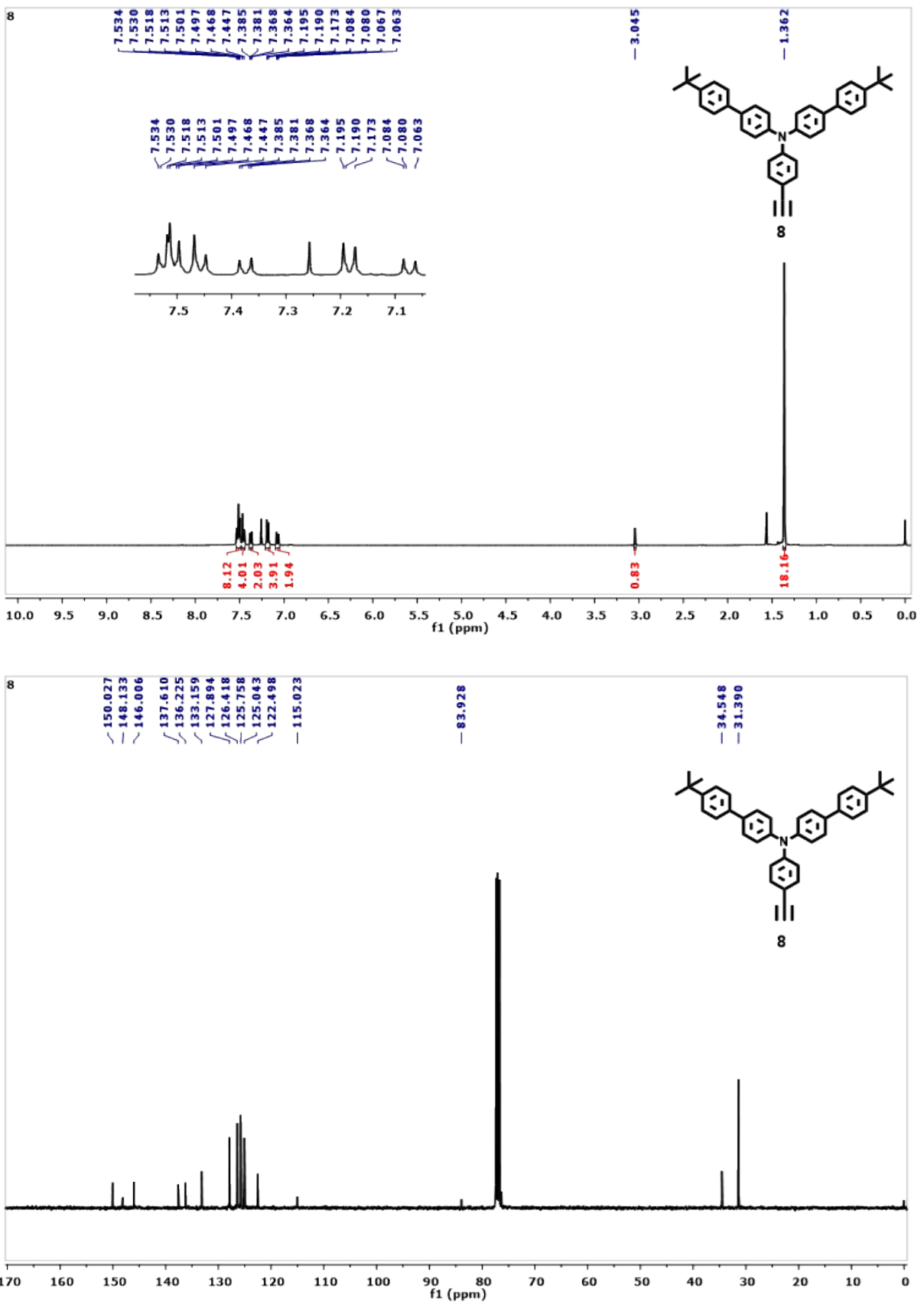


Figure S4: ^1H and ^{13}C NMR spectra of compound 8

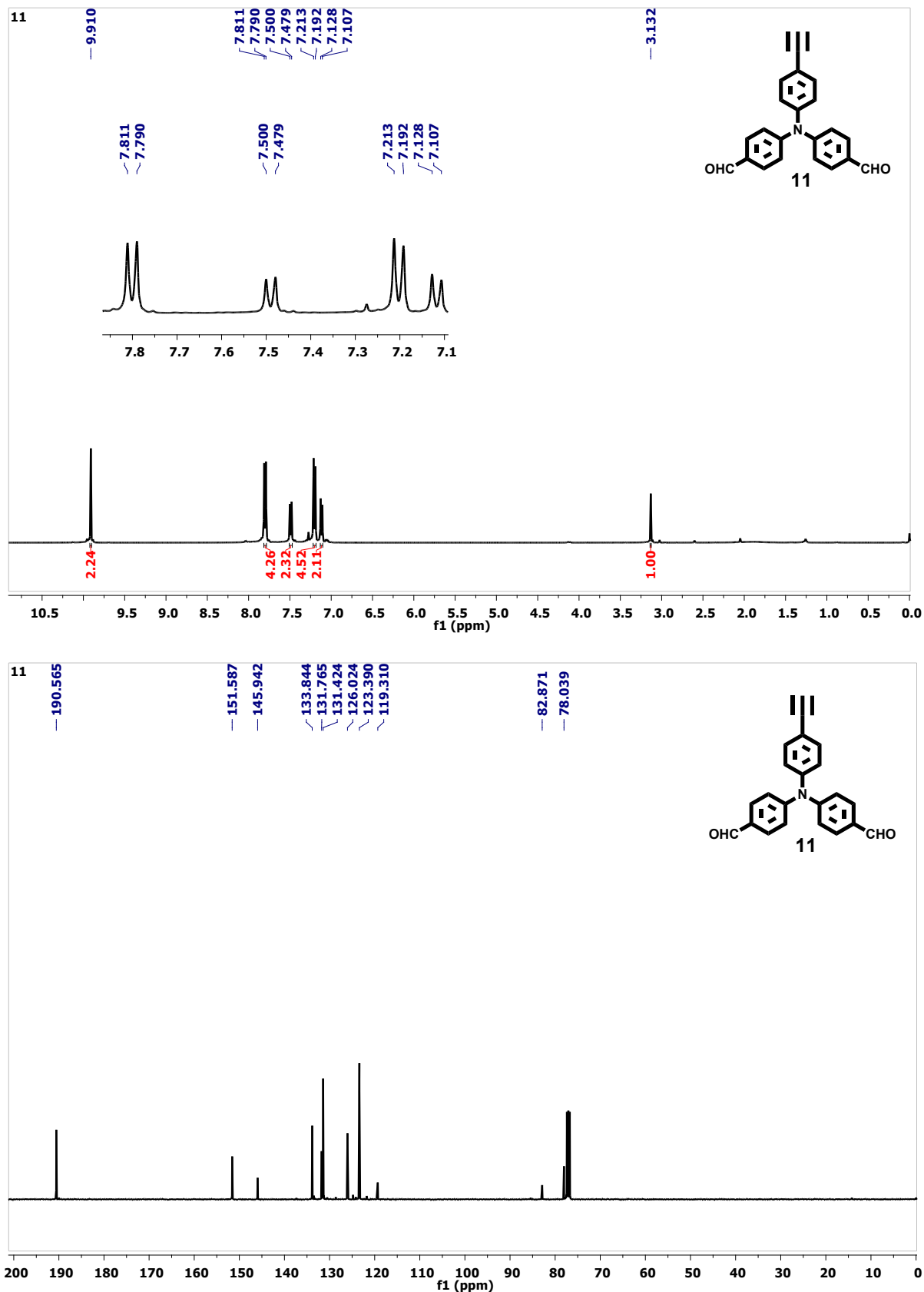
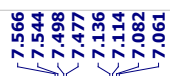


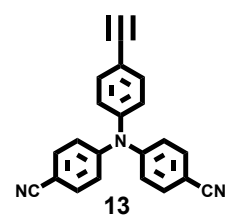
Figure S5: ^1H and ^{13}C NMR spectra of compound **11**

13



7.566
7.544
7.498
7.477
7.444
7.498
7.477
7.136
7.114
7.082
7.061

-3.130



7.8 7.7 7.6 7.5 7.4 7.3 7.2 7.1 7.0 6.9

4.37_{H1}
2.13_{H1}
4.47_{H1}
2.06_{H1}

1.00_{H1}

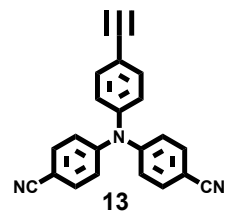
9.0 8.5 8.0 7.5 7.0 6.5 6.0 5.5 5.0 4.5 4.0 3.5 3.0 2.5 2.0 1.5 1.0 0.5 0.0

f1 (ppm)

13

-149.809
-145.436
<133.990
<133.718
125.935
<123.505
<119.667
<118.736

-106.556
-82.678
-78.224



170 160 150 140 130 120 110 100 90 80 70 60 50 40 30 20 10 0

f1 (ppm)

Figure S6: ^1H and ^{13}C NMR spectra of compound 13

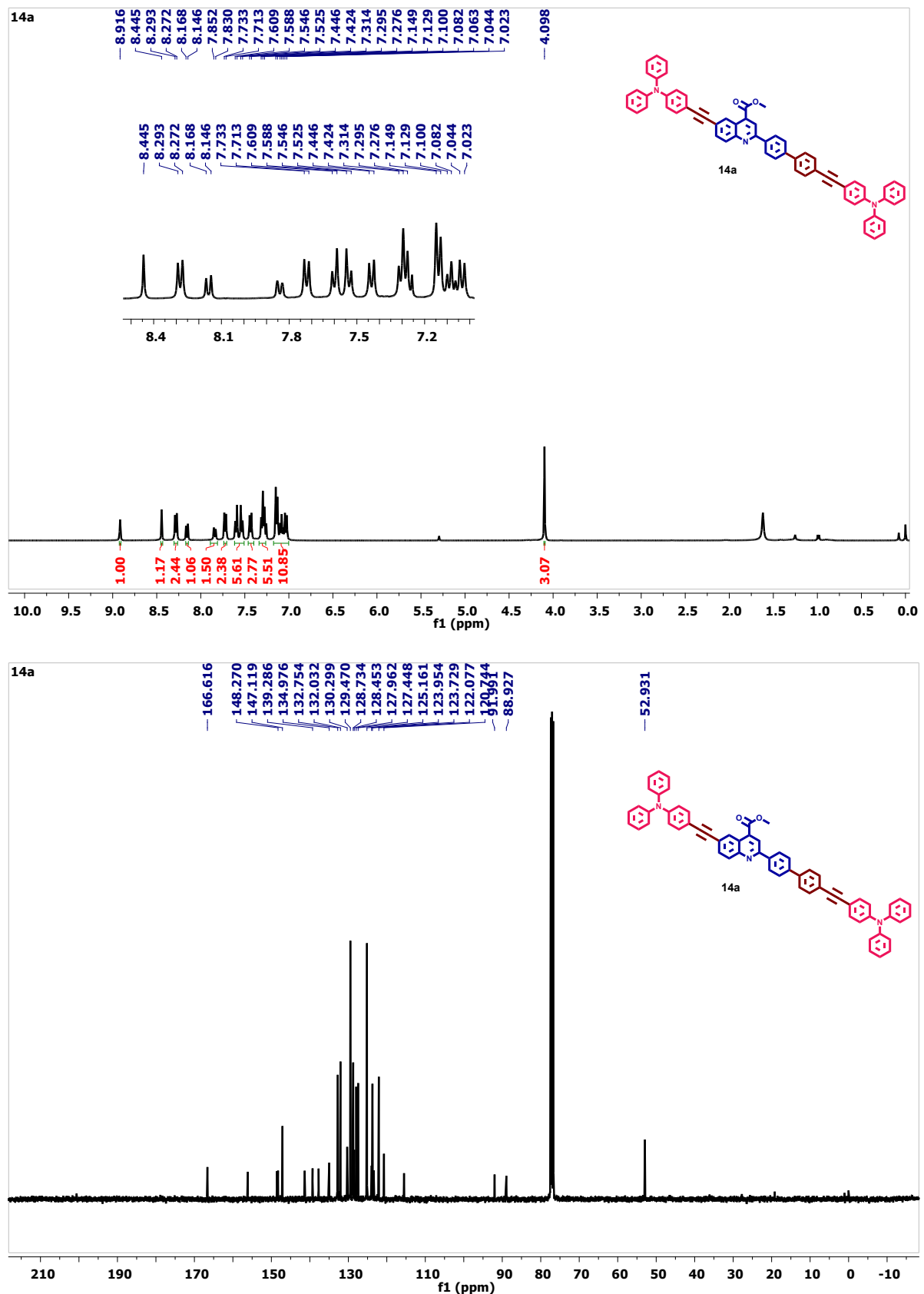


Figure S7: ¹H and ¹³C NMR spectra of compound 14a

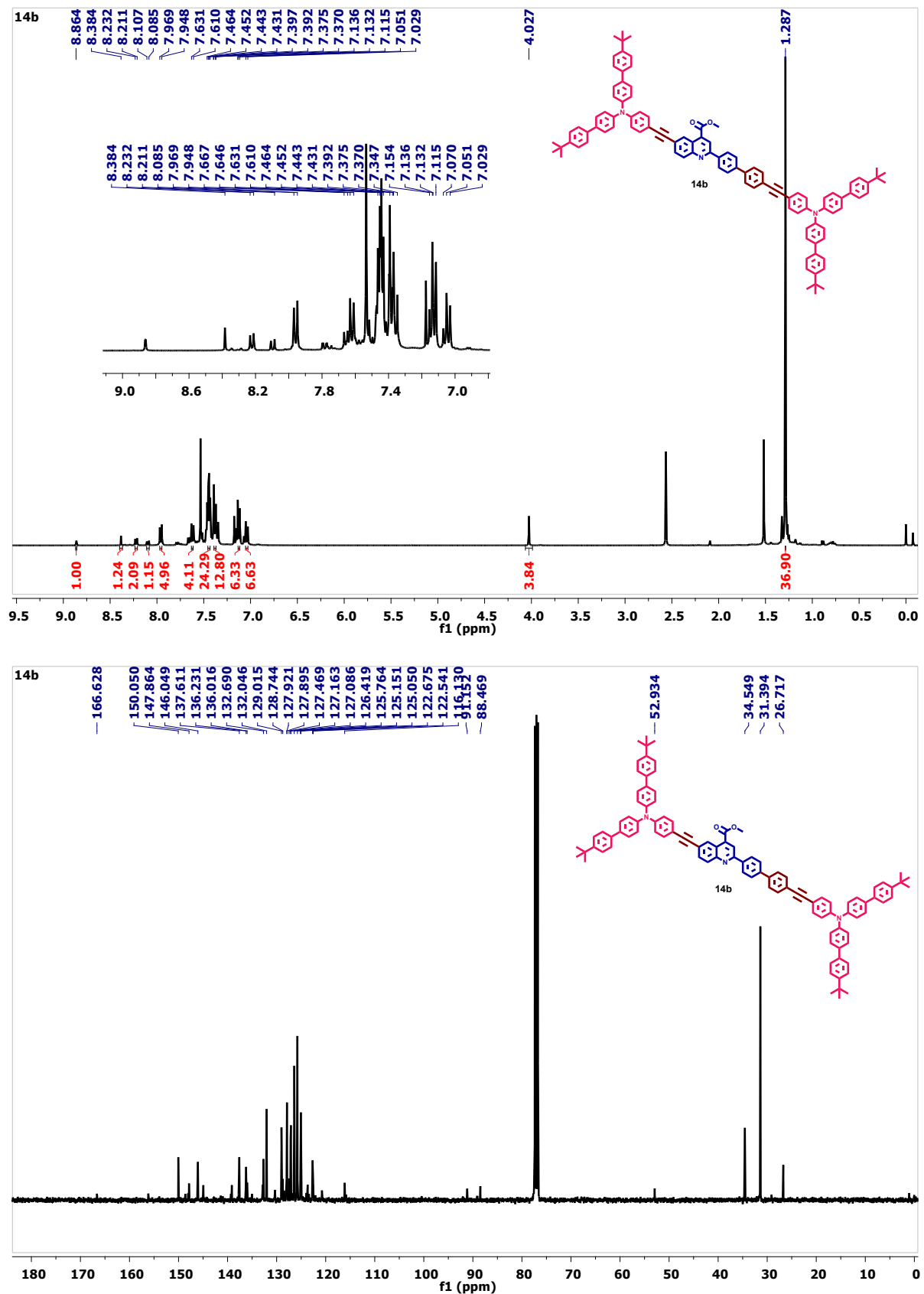


Figure S8: ¹H and ¹³C NMR spectra of compound 14b

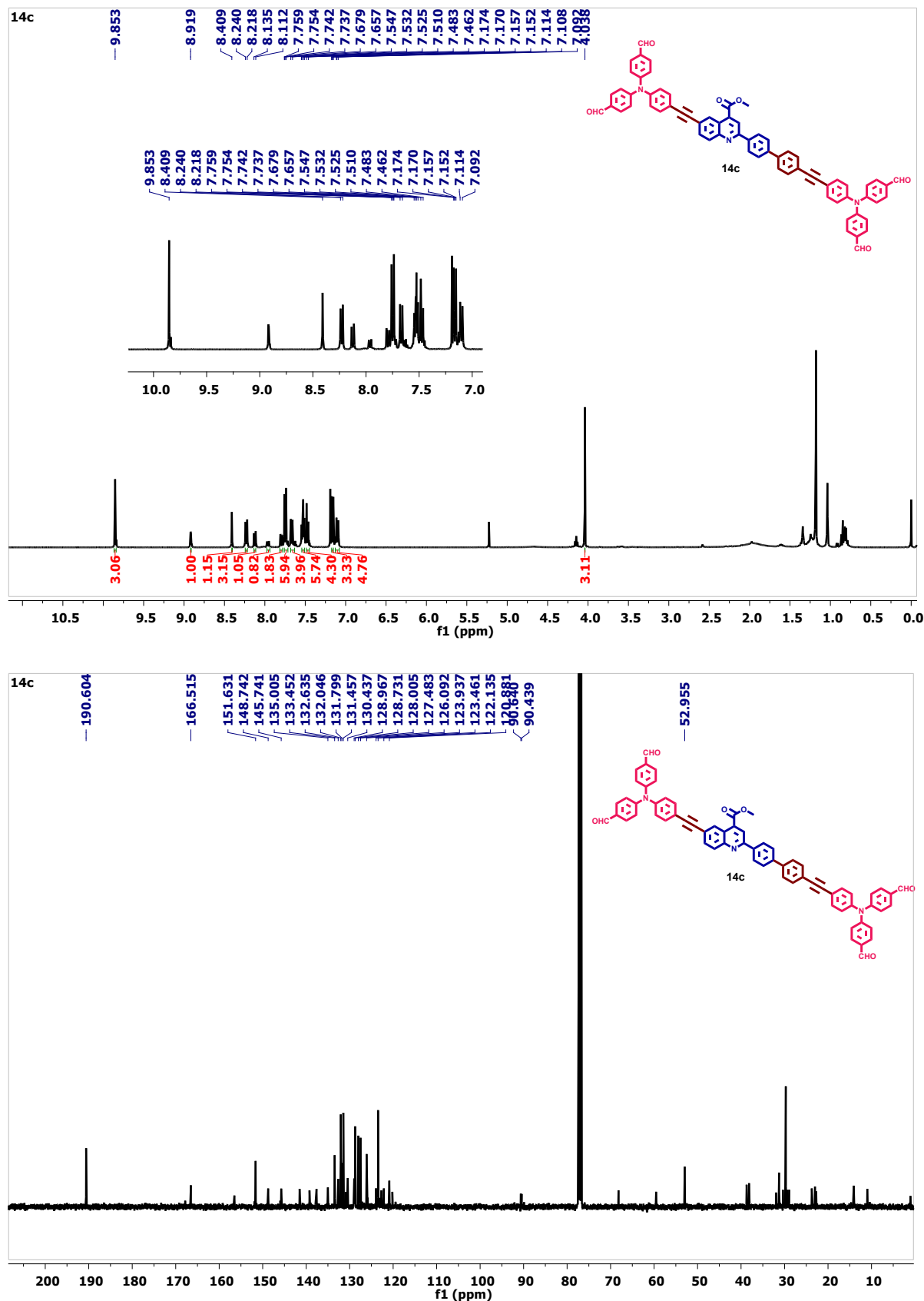


Figure S9: ¹H and ¹³C NMR spectra of compound 14c

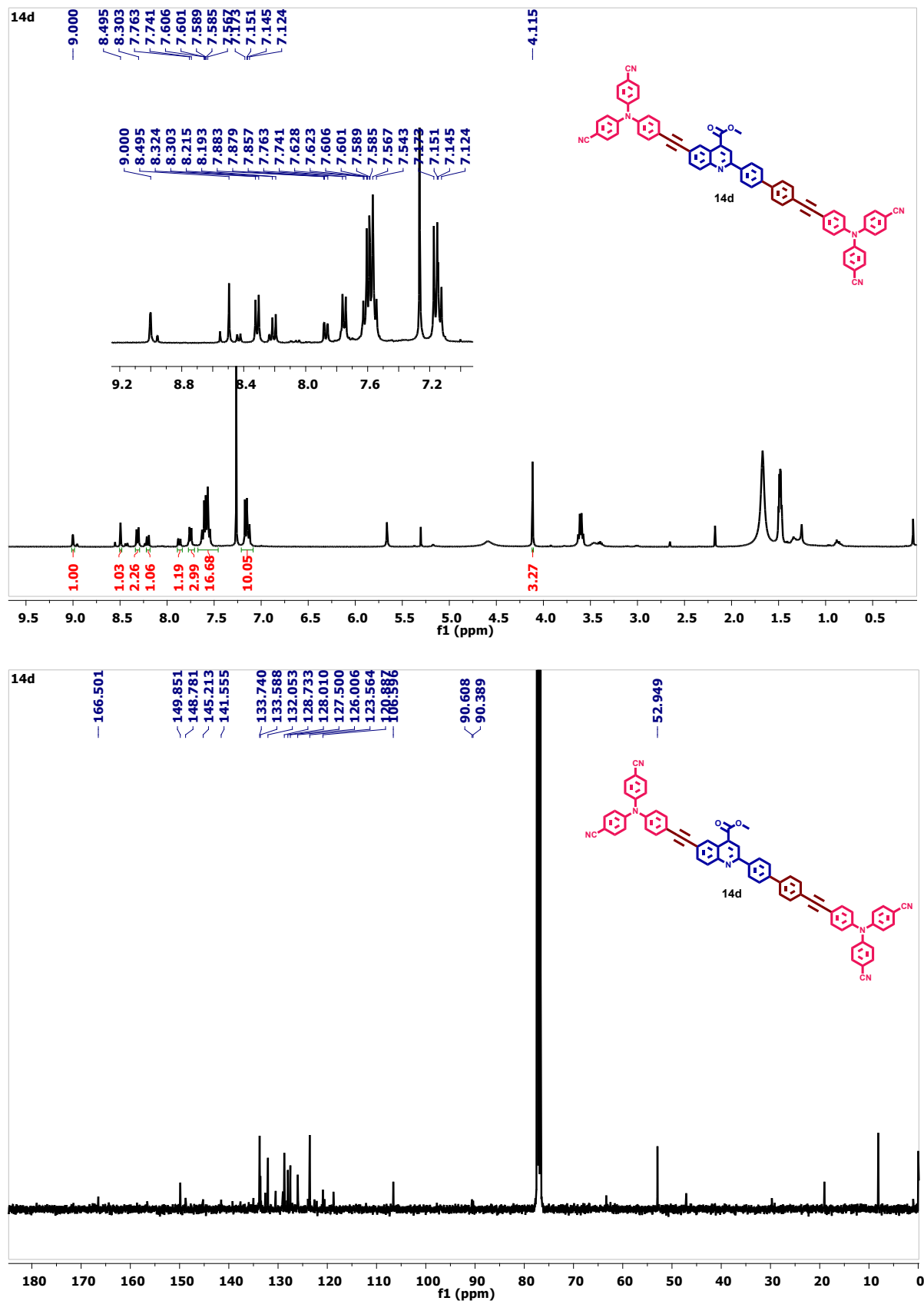


Figure S10: ¹H and ¹³C NMR spectra of compound 14d

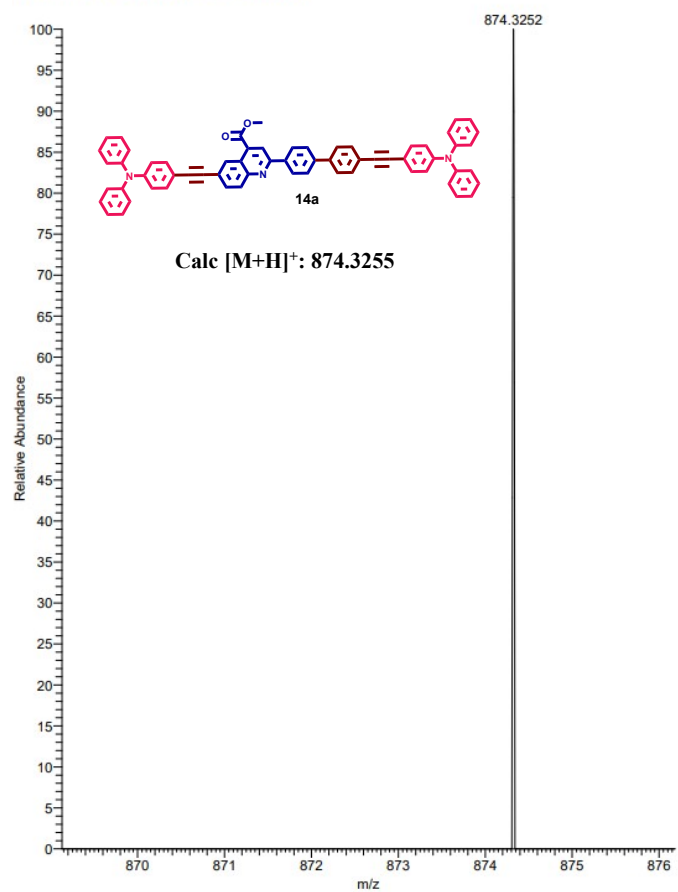


Figure S11: HRMS spectrum of compound **14a**

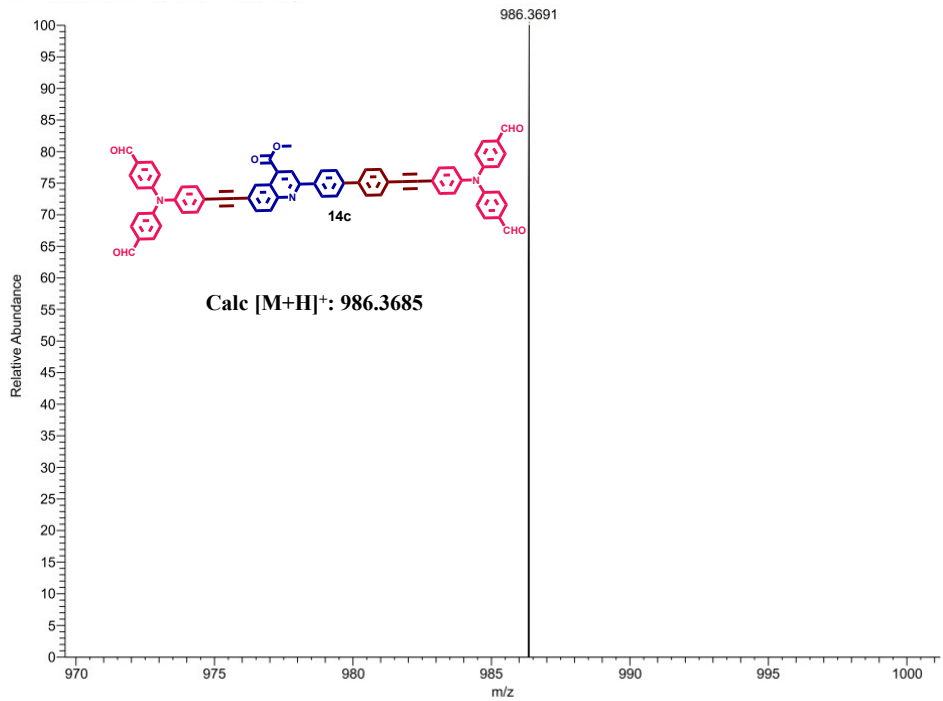


Figure S12: HRMS spectrum of compound **14c**

5. Thin film analysis of the compounds 14a-d

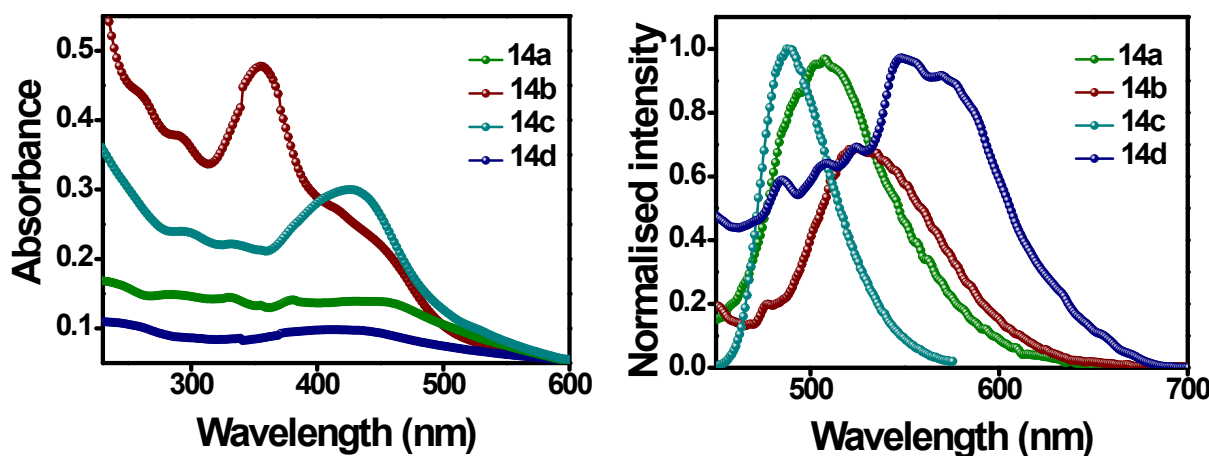


Figure S13: Thin-film absorption and emission spectra of the compounds 14a-d

6. Electrochemical studies of the compounds 14a-d

Cyclic voltammetry was used for investigating the electrochemical properties of the compounds by using the conventional three-electrode cell set up in which glassy carbon acts as the working electrode, platinum wire as the counter electrode, and standard calomel as the reference electrode (**Figure S14**). The experiments were carried out in anhydrous dimethylformamide solvent at room temperature with a scan rate of 100 mVs^{-1} where tetrabutylammonium hexafluorophosphate ($\text{n-Bu}_4\text{NPF}_6$, 0.1 M) was used as the supporting electrolyte. Nitrogen was purged to the solution to neglect any interference of oxygen with the compounds. Ferrocene/ferrocenium ion (Fc/Fc^+) redox couple was used for its calibration.²

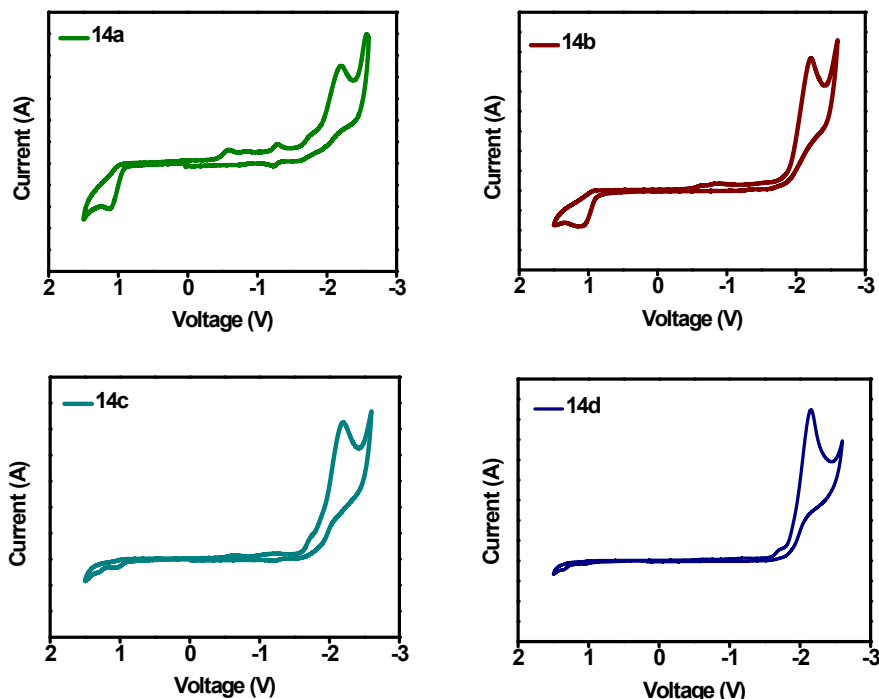


Figure S14: Cyclic voltammograms of the compounds 14a-d

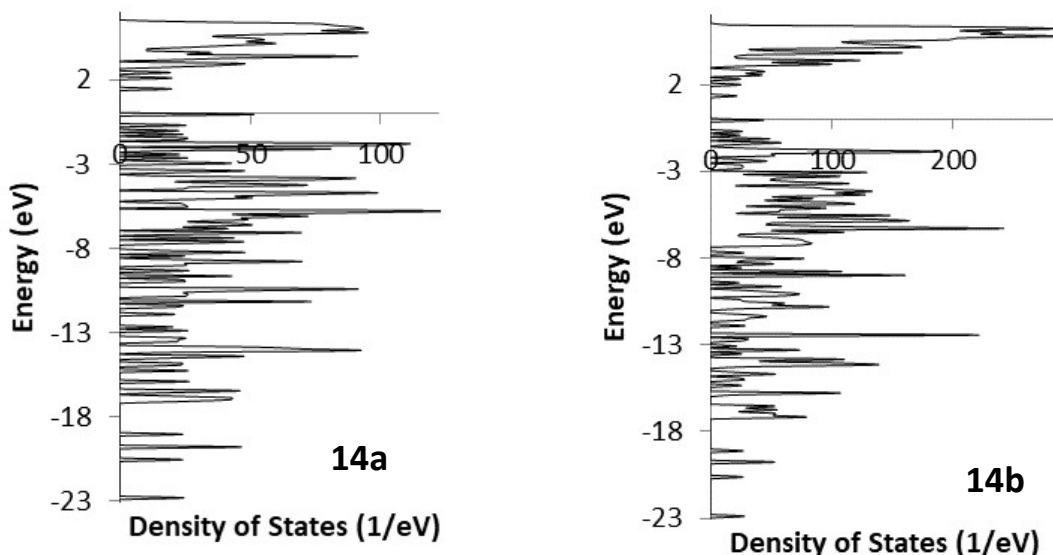
7. Computational studies on the compounds 9a-f

A series of computational simulations like Molecular Mechanics and semi-empirical methods were used to arrive at the plausible geometry of the structure as it is an important aspect for packing and predicting electronic properties of the system, some of which are usually non-covalent. The approximate geometrical parameters were then used to compute the optimized structure at the DFT's B3LYP level of theory and TD-SCF theoretically using Gaussian³. The excited states of the series of molecules were calculated by the computational methods and compared with experimentally obtained values (**Table S1**). The theoretical calculations using the TD-SCF (Time-Dependent SCF) suggest significant spectral insights. The emission bands found in the experimental methods are quite in agreement with the theoretical calculations. Out of the several values predicted by the theoretical methods only four values have been chosen that are closer to the experimental ones and that have a good frequency factor. The intersystem crossing has been predicted in almost all the systems and the values of emission spectra agree with these values.

Table S1: The predicted emission behavior of the compounds **14a-d**

Compound 14	Emission wavelength (nm)		Electronic transition	Dipole moment (D)
	Exp.	Comp.		
a	567.3	523.8	S ₀ -S ₁	1.2794
b	558.6	542.7	S ₀ -S ₁	1.1599
c	508.3	498.1	S ₁ -T ₂	4.5904
d	471.3	470.6	S ₀ -S ₁	2.6809

The DOS graph represents the number of states which offer high space for particle movements. It can be seen that the higher number of states are represented for the molecules **14a**, **14b**, and **14d** which are bigger, and are thus densely populated (**Figure S15**). As they are highly conjugated, the amount of the levels of DOS might be averaged.



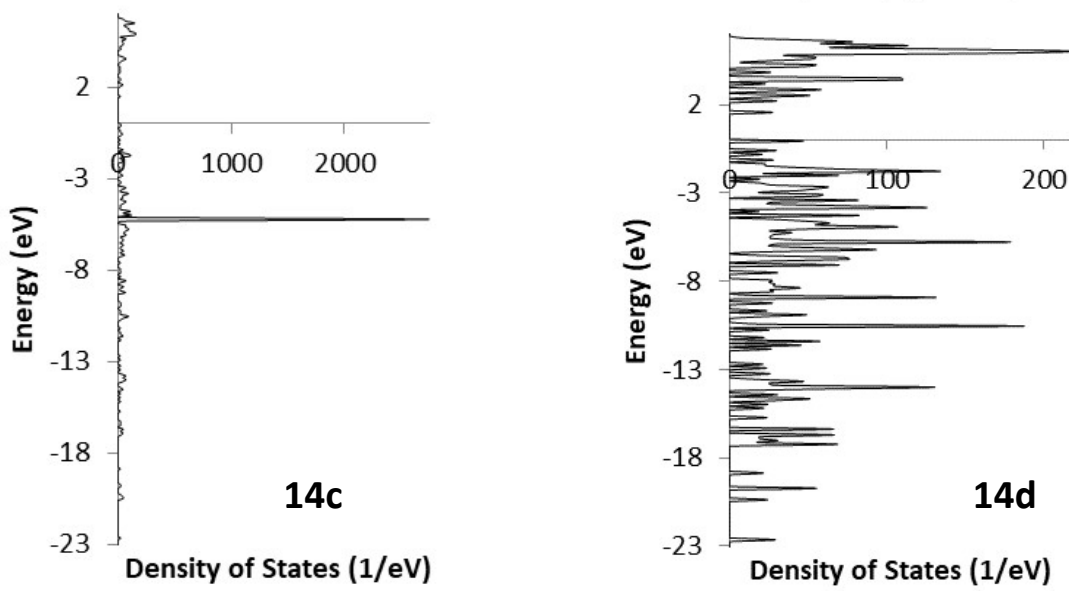


Figure S15: Density of states graphs for compounds **14a-d**

Table S2: DOS gap and E-Fermi energy of the molecules **14a-d**

S No	Molecular Formula	Free Energy (eV)	Density (Mg/m ³)	DOS Gap (eV)	E-Fermi (eV)
14a	C ₆₃ N ₃ O ₂ H ₄₃	-760.04	0.214	1.400	-3.765
14b	C ₁₀₃ N ₃ O ₂ H ₉₁	-1299.81	0.141	1.291	-3.949
14c	C ₆₇ N ₃ O ₆ H ₄₃	-821.68	0.220	1.407	-4.151
14d	C ₆₇ N ₇ O ₂ H ₃₉	-811.22	0.185	1.512	-4.362

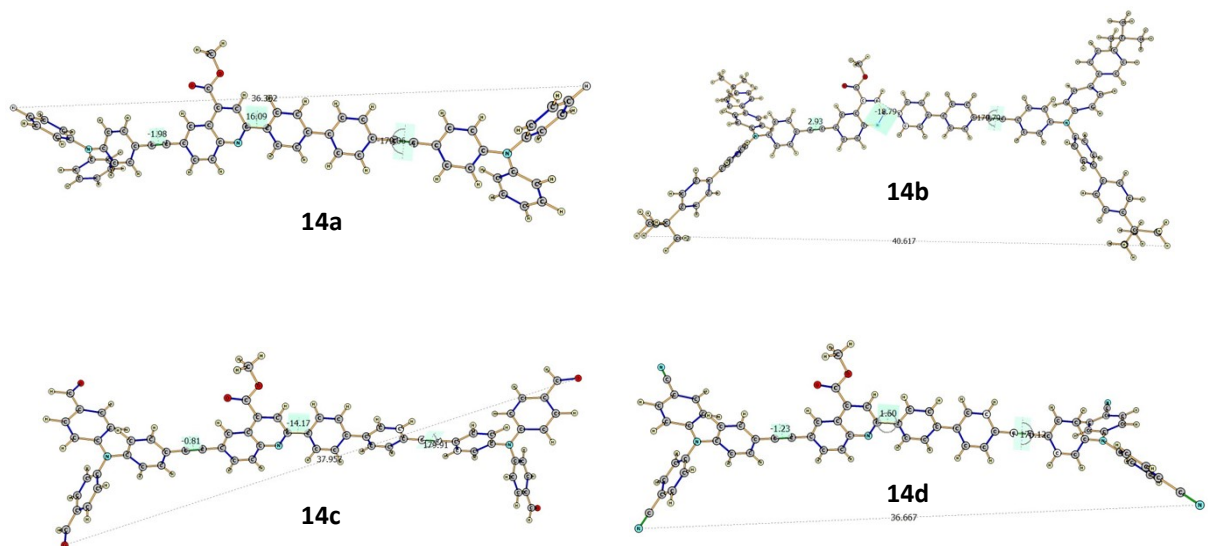


Figure S16: Optimised geometry of the compounds **14a-d**

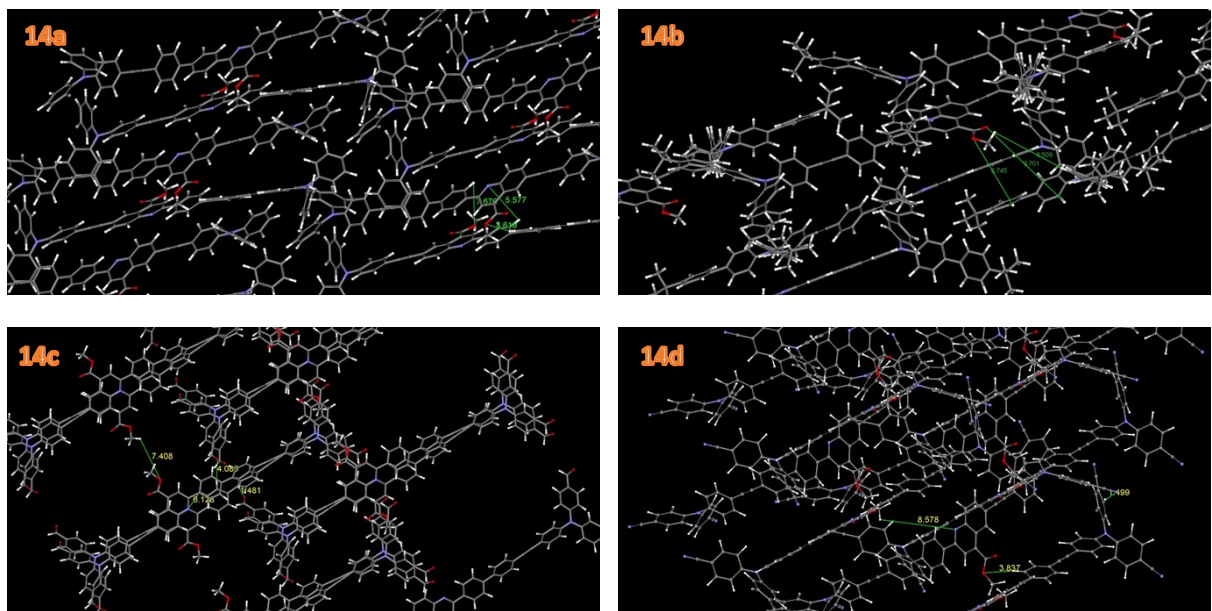


Figure S17: Molecular packing and hopping distances for the compounds **14a-d** through computational methods

Table S3: Hopping distance of molecules **14a-d** from computational data

Compound	Hopping distances (A°)
14a	3.619
	5.577
	7.676
14b	6.745
	8.509
	9.701
14c	4.086
	6.128
	7.408
14d	1.499
	3.837
	8.578

8. Memory device characterizations

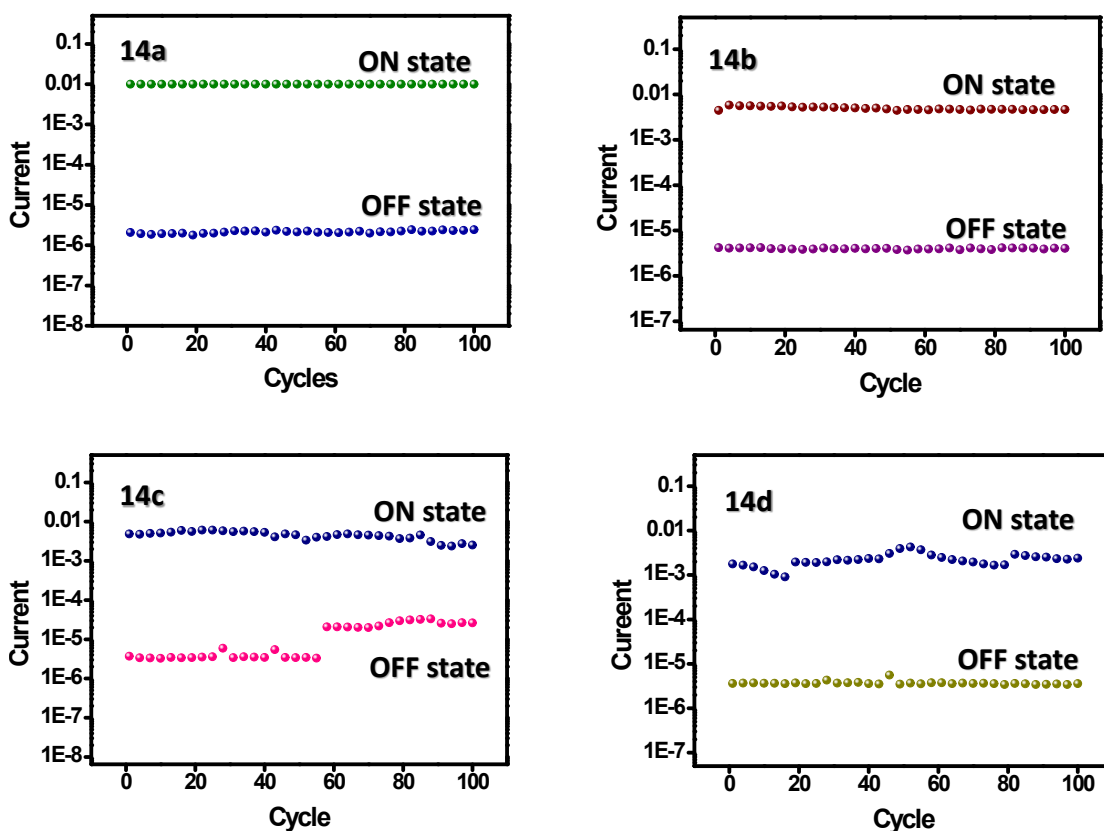


Figure S18: Endurance cycle of the memory devices **14a-d** under the constant stress of -0.5V

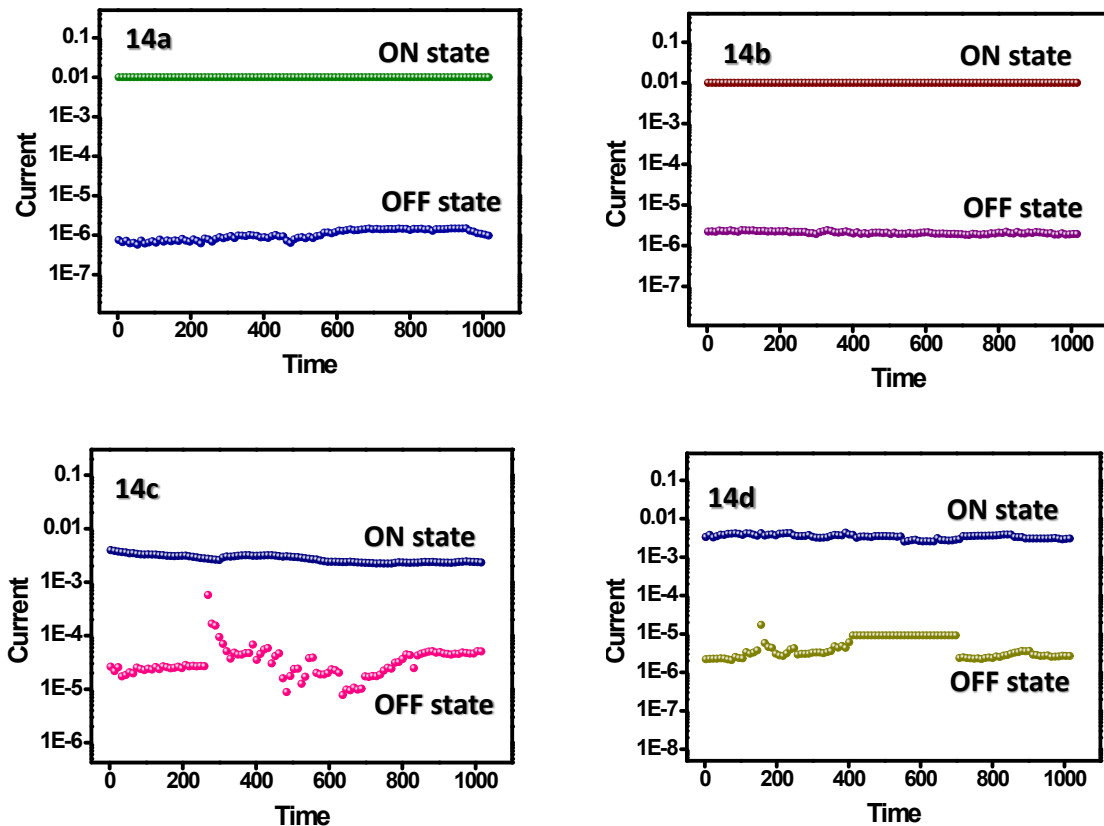


Figure S19: Retention time of the memory devices 14a-d under the constant stress of -0.5 V

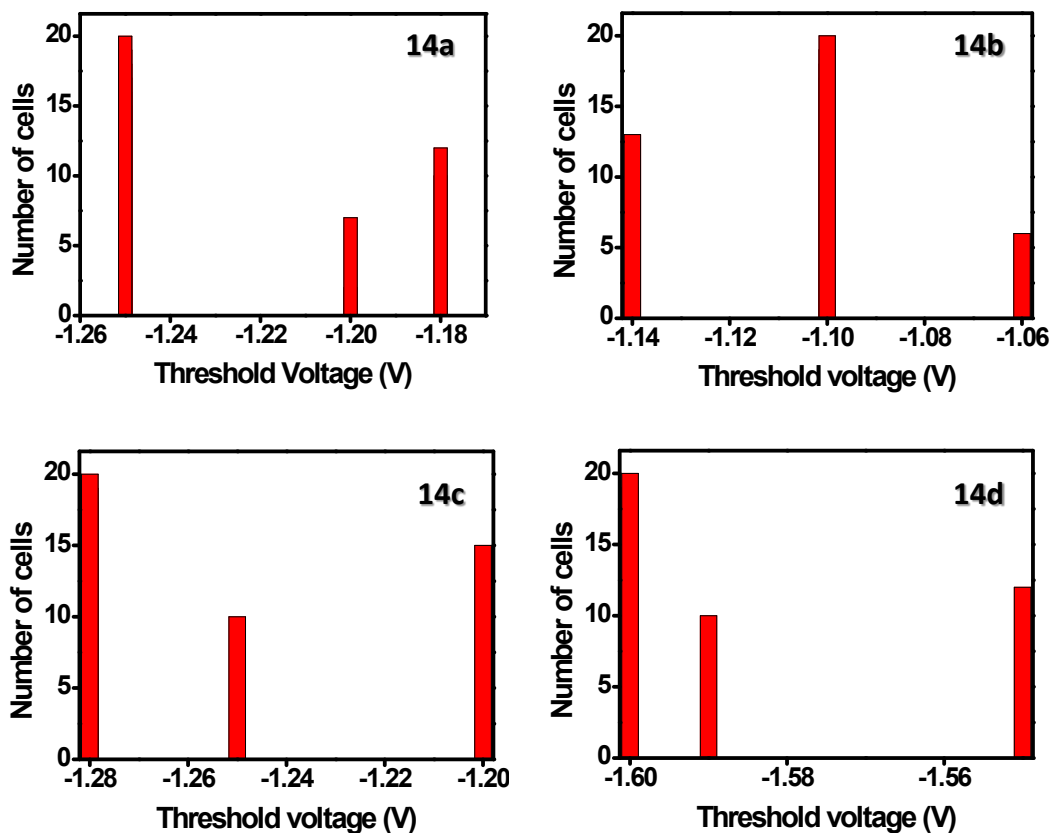


Figure S20: Threshold voltage distribution of the memory devices 14a-d

References

1. P. Devibala, R. Dheepika, P. Vadivelu and S. Nagarajan, Synthesis of Aroylbenzoate-Based Push-Pull Molecules for OFET Applications, *ChemistrySelect*, 2019, **4**, 2339–2346.
2. N. Elgrishi, K. J. Rountree, B. D. McCarthy, E. S. Rountree, T. T. Eisenhart and J. L. Dempsey, A Practical Beginner's Guide to Cyclic Voltammetry, *J. Chem. Educ.*, 2018, **95**, 197–206.
- 3 Frisch, M. J.; Tucks, G. W.; Schlegel, H. B.; Scuseria, G. E.; Robb, M. A.; Cheeseman, J. R.; Scalmani, G.; Barone, V.; Mennucci, B.; Petersson, G. A.; Nakatsuji, H.; Caricato, M.; Li, X.; Hratchian, H. P.; Izmaylov, A. F.; Bloino, J.; Zheng, G.; Sonnenberg, J. L.; Hada, M.; Ehara, M.; Toyota, K.; Fukuda, R.; Hasegawa, J.; Ishida, M.; Nakajima, T.; Honda, Y.; Kitao, O.; Nakai, H.; Vreven, T.; Montgomery, J. A.; Peralta, J. E.; Ogliaro, F.; Bearpark, M.; Heyd, J. J.; Brothers, E.; Kudin, K. N.; Staroverov, V. N.; Kobayashi, R.; Normand, J.; Raghavachari, K.; Rendell, A.; Burant, J. C.; Iyengar, S. S.; Tomasi, J.; Cossi, M.; Rega, N.; Millam, N. J.; Klene, M.; Knox, J. E.; Cross, J. B.; Bakken, V.; Adamo, C.; Jaramillo, J.; Gomperts, R.; Stratmann, R. E.; Yazyev, O.; Austin, A. J.; Cammi, R.; Pomelli, C.; Ochterski, J. W.; Martin, R. L.; Morokuma, K.; Zakrzewski, V. G.; Voth, G. A.; Salvador, P.; Dannenberg, J. J.; Dapprich, S.; Daniels, A. D.; Farkas, O.; Foresman, J. B.; Ortiz, J. V.; Cioslowski, J.; Fox, D. J.. Gaussian 09, revision A.1; Gaussian, Inc.: Wallingford, CT, 200.